

Effective field theory for triaxially deformed odd-mass nuclei

Q. B. Chen,^{1,*} N. Kaiser,^{1,†} Ulf-G. Meißner,^{2,3,4,‡} and J. Meng^{5,6,§}

¹*Physik-Department, Technische Universität München, D-85747 Garching, Germany*

²*Helmholtz-Institut für Strahlen- und Kernphysik and Bethe Center for Theoretical Physics,
Universität Bonn, D-53115 Bonn, Germany*

³*Institute for Advanced Simulation,
Institut für Kernphysik and Jülich Center for Hadron Physics,
Forschungszentrum Jülich, D-52425 Jülich, Germany*

⁴*Ivane Javakhishvili Tbilisi State University, 0186 Tbilisi, Georgia*

⁵*State Key Laboratory of Nuclear Physics and Technology,
School of Physics, Peking University, Beijing 100871, China*

⁶*Yukawa Institute for Theoretical Physics,
Kyoto University, Kyoto 606-8502, Japan*

(Dated: March 10, 2020)

Abstract

The effective field theory for collective rotations of triaxially deformed nuclei is generalized to odd-mass nuclei by including the angular momentum of the valence nucleon as an additional degree of freedom. The Hamiltonian is constructed up to next-to-leading order within the effective field theory formalism. The applicability of this Hamiltonian is examined by describing the wobbling bands observed in the lutetium isotopes ^{161,163,165,167}Lu. It is found that by taking into account the next-to-leading order corrections, quartic in the rotor angular momentum, the wobbling energies E_{wob} and spin-rotational frequency relations $\omega(I)$ are better described than with the leading order Hamiltonian.

*Electronic address: qbchen@pku.edu.cn

†Electronic address: nkaiser@ph.tum.de

‡Electronic address: meissner@hiskp.uni-bonn.de

§Electronic address: mengj@pku.edu.cn

I. INTRODUCTION

In Refs. [1, 2], an effective field theory (EFT) has been established to describe the rotational and vibrational motions of triaxially deformed even-even nuclei. The applicability of the EFT Hamiltonian at leading order (LO) and next-to-leading order (NLO) has been verified through a satisfactory description of the energy spectra of ground state bands, γ -bands, and $K = 4$ bands in the ruthenium isotopes $^{102-112}\text{Ru}$.

EFT is an approach based on symmetry principles alone, and it exploits the separation of scales for the systematic construction of the Hamiltonian supplemented by a power counting. In this way, an increase in the number of parameters (i.e., low-energy constants that need to be adjusted to data) goes hand in hand with an increase in precision and thereby counterbalances the partial loss of predictive power. Moreover, EFT often exhibits an impressive efficiency as highlighted by analytical results and economical means of calculations. In recent decades, chiral effective field theory has enjoyed considerable success in low-energy hadronic and nuclear structure physics. Pertinent examples include the descriptions of the nuclear forces [3–5], halo nuclei [6–8], and few-body systems [9–12].

Papenbrock and collaborators have presented a series of works on an EFT for axially deformed nuclei with the aim to investigate their rotational and vibrational excitations [13–20]. As mentioned at the beginning, we have extended this framework to triaxially deformed even-even nuclei [1, 2]. In the present work, we will further generalize the EFT to odd-mass nuclei with the aim to investigate their characteristic wobbling motion.

The wobbling motion, first proposed by Bohr and Mottelson in the 1970s [21], can occur only in a triaxially deformed nucleus and hence becomes a unique fingerprint of the triaxial nuclear shape. It manifests itself as an irregular precession of the rotational axis around the axis with the largest moment of inertia (MoI). The energy spectra related to this collective mode are called wobbling bands, which consist of sequences of $\Delta I = 2$ rotational bands built on different wobbling-phonon excitations [21].

For an odd-mass nucleus, the presence of the extra valence nucleon will affect the wobbling mode. Depending on the relative orientation between the quasi-particle angular momentum \mathbf{j} and the (intermediate) axis of the rotor with the largest MoI, two kinds of wobbling motion have been proposed by Frauendorf and Dönau [22]. If \mathbf{j} is aligned parallel, one speaks of *longitudinal* wobbling, where the wobbling energy increases with the spin I . If the alignment

is perpendicular, this mode is called *transverse* wobbling, and the corresponding wobbling energy decreases with the spin I .

Transverse wobbling bands have been reported in the mass region $A \approx 160$ for the isotopes ^{161}Lu [23], ^{163}Lu [24, 25], ^{165}Lu [26], ^{167}Lu [27], and ^{167}Ta [28], in the mass region $A \approx 130$ for ^{135}Pr [29, 30], and in the mass region $A \approx 100$ for ^{105}Pd [31]. In this list, ^{105}Pd represents the first odd-neutron nucleus for which (transverse) wobbling has been observed. In addition, transverse wobbling bands based on a two-quasiparticle configuration have been reported and studied for the even-even nucleus ^{130}Ba [32, 33]. On the other hand, longitudinal wobbling bands are rare and have been observed up to now only in the isotopes ^{133}La [34] and ^{187}Au [35].

In this paper, we will first extend the EFT description of the collective rotational motion of odd-mass nuclei by including the angular momentum of the valence nucleon as a relevant degree of freedom. The obtained Hamiltonian at NLO is applied to describe the wobbling bands in the lutetium isotopes $^{161,163,165,167}\text{Lu}$. We also consider the corresponding inter-band and intra-band electromagnetic transitions.

II. THEORETICAL FRAMEWORK

In this section, the procedure of constructing the effective Lagrangian and Hamiltonian for collective rotations of triaxially deformed odd-mass nuclei is outlined. It follows similar steps as in the case of collective rotations of even-even triaxially deformed nuclei investigated in Refs. [1, 2].

A. Dynamical variables

In an EFT, the symmetry is typically realized nonlinearly, and the Nambu-Goldstone fields parametrize the coset space \mathcal{G}/\mathcal{H} , where \mathcal{G} is the symmetry group of the Hamiltonian, and \mathcal{H} , the symmetry group of the ground state, is a proper subgroup of \mathcal{G} [36, 37]. The effective Lagrangian is built from those invariants that can be constructed from the fields in the coset space. A triaxial nucleus is invariant under $D_2 = Z_2 \times Z_2$ (generated by rotations about the body-fixed axes with an angle π), while $\text{SO}(3)$ symmetry is broken by the deformation. Hence, the Nambu-Goldstone modes lie on the three-dimensional coset

space $\text{SO}(3)/\text{D}_2$ [1, 2].

We write the Nambu-Goldstone fields in the body-fixed frame, where the three generators of infinitesimal rotations about the body-fixed 1, 2, and 3-axes are J_1 , J_2 , and J_3 . The modes depend on three time-dependent Euler angles $\alpha(t)$, $\beta(t)$, and $\gamma(t)$ that parametrize the unitary transformations $U(\alpha, \beta, \gamma)$ related to $\text{SO}(3)$ rotations in the following way:

$$U(\alpha, \beta, \gamma) = \exp\{-i\alpha(t)J_3\} \exp\{-i\beta(t)J_2\} \exp\{-i\gamma(t)J_3\}. \quad (1)$$

Note that the purely time-dependent variables $\alpha(t)$, $\beta(t)$, and $\gamma(t)$ correspond to the zero modes of the system. They parametrize rotations of the deformed nucleus and upon quantization they generate the rotational bands. Apparently, one is dealing here with a field theory in zero space-dimensions, i.e., ordinary quantum mechanics.

The underlying power counting is specified by

$$\alpha, \beta, \gamma \sim \mathcal{O}(1), \quad \dot{\alpha}, \dot{\beta}, \dot{\gamma} \sim \xi, \quad (2)$$

where the small parameter ξ denotes the energy scale of the rotational motion and the dot refers to a time derivative.

B. Building blocks

The effective Lagrangian is built from invariants. These are constructed from the components a_t^1 , a_t^2 , and a_t^3 of the angular velocity arising from the decomposition

$$U^{-1}i\partial_t U = a_t^1 J_1 + a_t^2 J_2 + a_t^3 J_3. \quad (3)$$

By taking appropriate traces of the matrix-exponentials, the expansion coefficients read

$$a_t^1 = -\dot{\alpha} \sin \beta \cos \gamma + \dot{\beta} \sin \gamma, \quad (4)$$

$$a_t^2 = \dot{\alpha} \sin \beta \sin \gamma + \dot{\beta} \cos \gamma, \quad (5)$$

$$a_t^3 = \dot{\alpha} \cos \beta + \dot{\gamma}. \quad (6)$$

One recognizes that these are the components of the angular velocity of the nucleus in the body-fixed frame, according to rigid-body kinematics [38].

C. Effective Lagrangian

Using the above building blocks, we have constructed in Ref. [1] the effective Lagrangian for the collective rotational motion of triaxially deformed even-even nuclei at LO (up to ξ^2)

$$\mathcal{L}_{\text{LO}}^{\text{ee}} = \frac{\mathcal{J}_1}{2}(a_t^1)^2 + \frac{\mathcal{J}_2}{2}(a_t^2)^2 + \frac{\mathcal{J}_3}{2}(a_t^3)^2, \quad (7)$$

and at NLO (up to ξ^4)

$$\begin{aligned} \mathcal{L}_{\text{NLO}}^{\text{ee}} = \mathcal{L}_{\text{LO}}^{\text{ee}} &+ \frac{\mathcal{M}_1}{4}(a_t^1)^4 + \frac{\mathcal{M}_2}{4}(a_t^2)^4 + \frac{\mathcal{M}_3}{4}(a_t^3)^4 \\ &+ \frac{\mathcal{M}_4}{2}(a_t^2)^2(a_t^3)^2 + \frac{\mathcal{M}_5}{2}(a_t^1)^2(a_t^3)^2 + \frac{\mathcal{M}_6}{2}(a_t^1)^2(a_t^2)^2, \end{aligned} \quad (8)$$

with \mathcal{J}_k ($k = 1 \dots 3$) and \mathcal{M}_k ($k = 1 \dots 6$) the parameters of moments of inertia to be determined from experimental data.

For an odd-mass nucleus, the extra degrees of freedom provided by the valence nucleon must be included in the Lagrangian. Similar to Ref. [13], we couple the angular momentum component j_k of valence nucleon to the Nambu-Goldstone modes a_t^k as

$$\mathcal{L}_C = j_1 a_t^1 + j_2 a_t^2 + j_3 a_t^3, \quad (9)$$

which has the form of a Coriolis interaction [21, 39].

Hence, the corresponding LO and NLO Lagrangians for collective rotation of odd-mass nuclei can be written as

$$\mathcal{L}_{\text{LO}}^{\text{eo}} = \mathcal{L}_{\text{LO}}^{\text{ee}} + \mathcal{L}_C, \quad (10)$$

$$\mathcal{L}_{\text{NLO}}^{\text{eo}} = \mathcal{L}_{\text{NLO}}^{\text{ee}} + \mathcal{L}_C. \quad (11)$$

Next, the corresponding Hamiltonians will be derived from these Lagrangians.

D. Effective Hamiltonian

We first derive the effective Hamiltonian at LO. From the LO Lagrangian $\mathcal{L}_{\text{LO}}^{\text{eo}}$, one obtains the canonical momenta as:

$$\begin{aligned} p_\alpha = \frac{\partial \mathcal{L}_{\text{LO}}^{\text{eo}}}{\partial \dot{\alpha}} &= -(a_t^1 \mathcal{J}_1 + j_1) \sin \beta \cos \gamma + (a_t^2 \mathcal{J}_2 + j_2) \sin \beta \sin \gamma \\ &+ (a_t^3 \mathcal{J}_3 + j_3) \cos \beta, \end{aligned} \quad (12)$$

$$p_\beta = \frac{\partial \mathcal{L}_{\text{LO}}^{\text{eo}}}{\partial \dot{\beta}} = (a_t^1 \mathcal{J}_1 + j_1) \sin \gamma + (a_t^2 \mathcal{J}_2 + j_2) \cos \gamma, \quad (13)$$

$$p_\gamma = \frac{\partial \mathcal{L}_{\text{LO}}^{\text{eo}}}{\partial \dot{\gamma}} = a_t^3 \mathcal{J}_3 + j_3. \quad (14)$$

Obviously, by dropping j_k in $a_t^k \mathcal{J}_k + j_k$, one gets back the canonical momenta in the case of an even-even nucleus written in Eqs. (8)-(10) of Ref. [1].

Using a Legendre transformation, the Hamiltonian is obtained as

$$\begin{aligned} \mathcal{H}_{\text{LO}}^{\text{eo}} &= \dot{\alpha} p_\alpha + \dot{\beta} p_\beta + \dot{\gamma} p_\gamma - \mathcal{L}_{\text{LO}} \\ &= \frac{1}{2\mathcal{J}_1} \left[\left(-\frac{\cos \gamma}{\sin \beta} p_\alpha + \sin \gamma p_\beta + \cos \gamma \cot \beta p_\gamma \right) - j_1 \right]^2 \\ &\quad + \frac{1}{2\mathcal{J}_2} \left[\left(\frac{\sin \gamma}{\sin \beta} p_\alpha + \cos \gamma p_\beta - \sin \gamma \cot \beta p_\gamma \right) - j_2 \right]^2 \\ &\quad + \frac{1}{2\mathcal{J}_3} \left[(p_\gamma) - j_3 \right]^2. \end{aligned} \quad (15)$$

Note that the expressions in the round brackets are the three components of the total angular momentum I_1 , I_2 , and I_3 with respect to the body-fixed frame [39],

$$I_1 = -\frac{\cos \gamma}{\sin \beta} p_\alpha + \sin \gamma p_\beta + \cos \gamma \cot \beta p_\gamma, \quad (16)$$

$$I_2 = \frac{\sin \gamma}{\sin \beta} p_\alpha + \cos \gamma p_\beta - \sin \gamma \cot \beta p_\gamma, \quad (17)$$

$$I_3 = p_\gamma. \quad (18)$$

Consequently, the Hamiltonian at LO reads

$$\mathcal{H}_{\text{LO}}^{\text{eo}} = \frac{(I_1 - j_1)^2}{2\mathcal{J}_1} + \frac{(I_2 - j_2)^2}{2\mathcal{J}_2} + \frac{(I_3 - j_3)^2}{2\mathcal{J}_3}, \quad (19)$$

and this formula represents the Hamiltonian of a triaxial rotor with angular momentum components $R_k = I_k - j_k$. Obviously, the rotor and quasi-particle angular momenta are coupled to the total angular momentum by $\mathbf{I} = \mathbf{R} + \mathbf{j}$.

Following a similar procedure, one derives the effective Hamiltonian at NLO as

$$\begin{aligned} \mathcal{H}_{\text{NLO}}^{\text{eo}} &= \mathcal{H}_{\text{LO}}^{\text{eo}} \\ &\quad - \frac{\mathcal{M}_1(I_1 - j_1)^4}{4\mathcal{J}_1^4} - \frac{\mathcal{M}_2(I_2 - j_2)^4}{4\mathcal{J}_2^4} - \frac{\mathcal{M}_3(I_3 - j_3)^4}{4\mathcal{J}_3^4} \\ &\quad - \frac{\mathcal{M}_4[(I_2 - j_2)^2(I_3 - j_3)^2 + (I_3 - j_3)^2(I_2 - j_2)^2]}{4\mathcal{J}_2^2\mathcal{J}_3^2} \\ &\quad - \frac{\mathcal{M}_5[(I_3 - j_3)^2(I_1 - j_1)^2 + (I_1 - j_1)^2(I_3 - j_3)^2]}{4\mathcal{J}_1^2\mathcal{J}_3^2} \end{aligned}$$

$$- \frac{\mathcal{M}_6[(I_1 - j_1)^2(I_2 - j_2)^2 + (I_2 - j_2)^2(I_1 - j_1)^2]}{4\mathcal{J}_1^2\mathcal{J}_2^2}. \quad (20)$$

Note that the last three terms have been written as anticommutators to guarantee a hermitean Hamiltonian. Again, by dropping the j_k one recovers the NLO effective Hamiltonian of the even-even rotor given in Eq. (36) of Ref. [1].

At this point, one needs also a Hamiltonian that describes the motion of the valence nucleon. Since it cannot be derived from the EFT concept based on Nambu-Goldstone modes, we borrow it from the phenomenologically successful Nilsson model in the form of a single- j shell Hamiltonian [21, 39]

$$h_p = \frac{C}{2} \left\{ \cos \gamma_2 \left[j_3^2 - \frac{j(j+1)}{3} \right] + \frac{\sin \gamma_2}{2\sqrt{3}} (j_+^2 + j_-^2) \right\}, \quad (21)$$

with γ_2 the triaxial deformation parameter. The coupling parameter C is related to the axial deformation parameter β_2 by [40]

$$C = \frac{123}{8} \sqrt{\frac{5}{\pi}} \frac{2N+3}{j(j+1)} A^{-1/3} \beta_2, \quad (22)$$

with N the oscillator quantum number of the major shell embedding the single- j shell, and A the mass number.

With this completion, the total rotational Hamiltonian for odd-mass nuclei reads

$$\mathcal{H}_{\text{LO}} = h_p + \mathcal{H}_{\text{LO}}^{\text{eo}}, \quad (23)$$

$$\mathcal{H}_{\text{NLO}} = h_p + \mathcal{H}_{\text{NLO}}^{\text{eo}}. \quad (24)$$

Note that \mathcal{H}_{LO} is nothing but the renowned particle-rotor model Hamiltonian [21, 39].

E. Solutions of the rotational Hamiltonian

The Hamiltonian can be solved by diagonalization in a complete basis. Here, we adopt the so-called weak-coupling basis [21, 39, 41, 42]

$$|IMjRK_R\rangle = \sum_{m, M_R} \langle jmRM_R|IM\rangle |jm\rangle \otimes |RM_RK_R\rangle, \quad (25)$$

where I denotes the total angular momentum quantum number of the odd-mass nuclear system (rotor plus particle). Furthermore, m , M_R , and M are the quantum numbers corresponding to the projections of \mathbf{j} , \mathbf{R} , and \mathbf{I} onto the 3-axis of the laboratory frame, and K_R

is related to the projection of \mathbf{R} onto the 3-axis of the principal axes frame. Obviously, the appearance of Clebsch-Gordan coefficients $\langle jmRM_R|IM\rangle$ requires $M = m + M_R$, and the values of R must satisfy the triangular condition $|I - j| \leq R \leq I + j$ of angular momentum coupling.

Making use of Wigner-functions, the rotational wave functions of the particle and the rotor in Eq. (25) can be written as

$$|jm\rangle = \sum_{\Omega=-j}^j D_{m\Omega}^j |j\Omega\rangle, \quad (26)$$

$$|RM_R K_R\rangle = \sqrt{\frac{2R+1}{16\pi^2(1+\delta_{K_R 0})}} \left[D_{M_R K_R}^R + (-1)^R D_{M_R - K_R}^R \right], \quad (27)$$

where Ω is the quantum number related to the 3-axis component of the particle angular momentum \mathbf{j} in the intrinsic frame. Furthermore, K_R is an even integer ranging from 0 to R , where $K_R = 0$ is excluded for odd R . Both restrictions on K_R come from the D_2 symmetry of a triaxial nucleus [21]. Note that for an axially symmetric nucleus, R can take only even integer values since K_R must be zero.

The matrix elements of the collective rotor Hamiltonian can now be calculated easily as

$$\langle IMjRK'_R | \mathcal{H}_{\text{LO/NLO}}^{\text{eo}} | IMjRK_R \rangle = \sum_i c_{K'_R}^{Ri} E_{Ri} c_{K_R}^{Ri}, \quad (28)$$

where the eigenenergies E_{Ri} and corresponding coefficients $c_{K_R}^{Ri}$ (i labels the different eigenstates) of the eigenvectors are obtained by diagonalizing the collective rotor Hamiltonian $\mathcal{H}_{\text{LO/NLO}}^{\text{eo}}$ in the basis $|RM_R K_R\rangle$ introduced in Eq. (27):

$$\mathcal{H}_{\text{LO/NLO}}^{\text{eo}} |RM_R i\rangle = E_{Ri} |RM_R i\rangle, \quad (29)$$

$$|RM_R i\rangle = \sum_{K_R} c_{K_R}^{Ri} |RM_R K_R\rangle. \quad (30)$$

F. Electromagnetic transitions

In general, the electromagnetic transition probability is calculated as [21, 39]

$$B(\sigma\lambda, I' \rightarrow I) = \frac{1}{2I' + 1} \sum_{\mu M'} |\langle IM | \mathcal{M}(\sigma\lambda, \mu) | I' M' \rangle|^2, \quad (31)$$

where $\mathcal{M}(\sigma\lambda, \mu)$ is the electromagnetic transition operator of multi-polarity $\sigma\lambda$, and $M = M' + \mu$.

In the present work, the rotational wave function $|IM\rangle$ is expanded in the weak-coupling basis (25) as

$$|IM\rangle = \sum_{R,K_R} c_{R,K_R} |IMjRK_R\rangle = \sum_{R,K_R,m} d_{m,R,K_R} |jm\rangle |RM_RK_R\rangle, \quad (32)$$

with $d_{m,R,K_R} = c_{R,K_R} \langle jmRM_R | IM \rangle$. Therefore, the electromagnetic transition probability can be rewritten as

$$B(\sigma\lambda, I' \rightarrow I) = \frac{1}{2I' + 1} \sum_{\mu M'} \left| \sum_{R',K'_R,m'} \sum_{R,K_R,m} d_{m,R,K_R} d_{m',R',K'_R} \right. \\ \left. \times \langle jm | \langle RM_RK_R | \mathcal{M}(\sigma\lambda, \mu) | jm' \rangle | R'M'_RK'_R \rangle \right|^2. \quad (33)$$

For an $E2$ transition, the corresponding operator is

$$\mathcal{M}(E2, \mu) = \sqrt{\frac{5}{16\pi}} Q_{2\mu}, \quad (34)$$

with the quadrupole moments in the laboratory frame

$$Q_{2\mu} = \sum_{\nu} D_{\mu\nu}^{2*} Q'_{2\nu}, \quad (35)$$

obtained by a rotation from the quadrupole moments in the principal axis frame

$$Q'_{20} = Q_0 \cos \gamma_2, \\ Q'_{21} = Q'_{2-1} = 0, \\ Q'_{22} = Q'_{2-2} = \frac{1}{\sqrt{2}} Q_0 \sin \gamma_2. \quad (36)$$

Here, $Q_0 = (3/\sqrt{5\pi}) R_0^2 Z \beta_2$ is the intrinsic quadrupole moment, with $R_0 = 1.2A^{1/3}$ the nuclear radius, and Z the charge number. Since $m' = m$ is required in Eq. (33) for $E2$ transition, one gets

$$B(E2, I' \rightarrow I) = \frac{1}{2I' + 1} \sum_{\mu M'} \left| \sum_{R,K_R,R',K'_R,m} d_{m,R,K_R} d_{m,R',K'_R} \right. \\ \left. \times \langle RM_RK_R | \mathcal{M}(E2, \mu) | R'M'_RK'_R \rangle \right|^2. \quad (37)$$

For a $M1$ transition, the operator $\mathcal{M}(M1, \mu)$ is composed of the particle and rotor angular momenta in the laboratory frame

$$\mathcal{M}(M1, \mu) = g_p \hat{j}_\mu + g_R \hat{R}_\mu$$

$$= g_R \hat{I}_\mu + (g_p - g_R) \hat{j}_\mu, \quad (38)$$

where g_p and g_R are the g -factors of particle and rotor. Note that since transition matrix elements of \hat{I}_μ vanish, the first term can be dropped. In the second term, \hat{j}_μ with $\mu = 0, \pm 1$ denotes the spherical components of the particle angular momentum,

$$\hat{j}_0 = j_3, \quad \hat{j}_{\pm 1} = \mp \frac{1}{\sqrt{2}}(j_1 \pm ij_2). \quad (39)$$

Now, one has in Eq. (33) the conditions $R' = R$, $M'_R = M_R$, and $K'_R = K_R$, and therefore the $M1$ transition probability simplifies to

$$B(M1, I' \rightarrow I) = \frac{1}{2I' + 1} \sum_{\mu M'} \left| \sum_{R, K_R, m, m'} d_{m, R, K_R} d_{m', R', K'_R} \right. \\ \left. \times \langle jm | \mathcal{M}(M1, \mu) | jm' \rangle \right|^2. \quad (40)$$

III. RESULTS AND DISCUSSION

In the calculations, the moment of inertia parameters \mathcal{J}_k and \mathcal{M}_k appearing in the LO and NLO Hamiltonian are fitted to the data. The deformation parameters for the single- j shell Hamiltonian (21) are taken from Ref. [24] as $\beta_2 = 0.40$ and $\gamma_2 = 20^\circ$.

A. Wobbling bands in ^{163}Lu

In Fig. 1, the energy differences with respect to the yrast band (called wobbling energies E_{wob}) of the first and second wobbling bands in ^{163}Lu as calculated in the EFT at LO and NLO are shown in comparison to the experimental data [24, 25]. In Fig. 2, the spin-rotational frequency relationships $\omega(I) = [E(I) - E(I - 2)]/2$ for the yrast band in ^{163}Lu as calculated in the EFT at LO and NLO are shown in comparison to the experimental data [24, 25]. For the various fits, the obtained parameters are listed in Table I.

In our EFT calculations, we have adopted four strategies of fitting (I)-(IV). In fit (I), the wobbling energies of the first wobbling band and the rotational frequencies of the yrast band are used to determine simultaneously the parameters \mathcal{J}_k and \mathcal{M}_k appearing in the EFT formalism. It is seen that the wobbling energies of the first wobbling band as well as the rotational frequencies of the yrast band can be reproduced. But the calculated wobbling

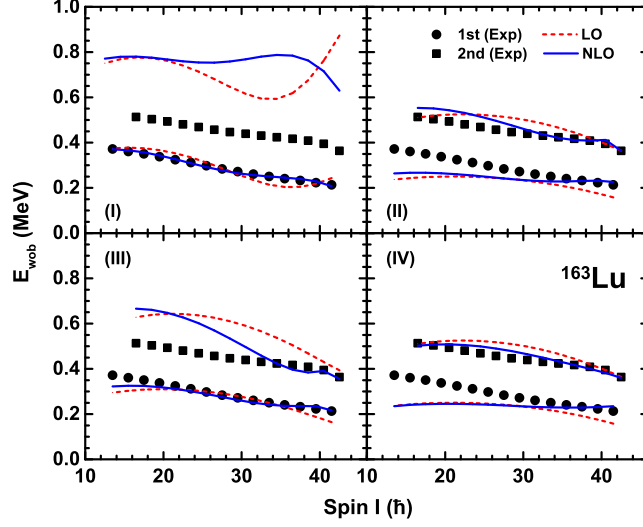


FIG. 1: (Color online) Wobbling energies of the first and second wobbling bands as functions of spin I in ^{163}Lu calculated at LO and NLO by four fitting strategies (I)-(IV) in comparison to the experimental data [24, 25].

energies of the second wobbling band are overpredicted by about 0.3 MeV with respect to the experimental values.

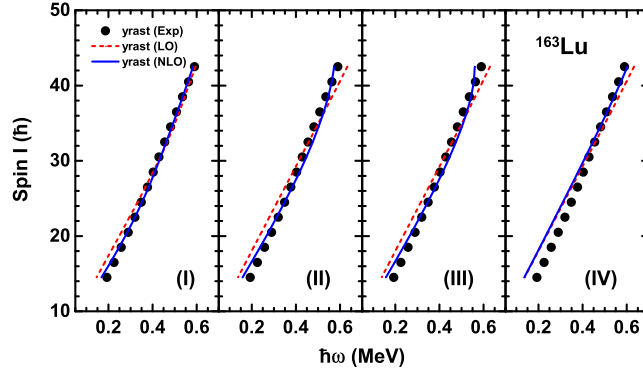


FIG. 2: (Color online) Spin-rotational frequency relationships for the yrast band in ^{163}Lu calculated at LO and NLO by four fitting strategies (I)-(IV) in comparison with experimental data [24, 25].

In fit (II), we have further included the wobbling energies of the second wobbling band to determine the parameters \mathcal{J}_k and \mathcal{M}_k . In this case, the description of the second wobbling band gets much improved. In particular, the calculated wobbling energies of the second wobbling band decrease with spin I . However, the wobbling energy of the first wobbling

band is underestimated about 0.1 MeV in the low spin region.

TABLE I: Parameters used in the LO and NLO calculations in four fitting strategies for ^{163}Lu . The units of \mathcal{J}_k and \mathcal{M}_k are \hbar^2/MeV and \hbar^4/MeV^3 , respectively.

| | Nucleus | (I) | (II) | (III) | (IV) |
|-----|-----------------|--------|-------|-------|--------|
| LO | \mathcal{J}_1 | 65.48 | 61.67 | 62.88 | 61.67 |
| | \mathcal{J}_2 | 50.51 | 55.46 | 55.02 | 55.46 |
| | \mathcal{J}_3 | 4.09 | 12.56 | 7.89 | 12.56 |
| NLO | \mathcal{J}_1 | 60.56 | 53.18 | 54.24 | 61.67 |
| | \mathcal{J}_2 | 44.45 | 47.13 | 47.08 | 56.46 |
| | \mathcal{J}_3 | 3.85 | 10.43 | 6.87 | 12.56 |
| | \mathcal{M}_1 | -4.93 | 19.99 | 19.99 | 18.44 |
| | \mathcal{M}_2 | 19.77 | 19.07 | 19.04 | 7.73 |
| | \mathcal{M}_3 | -0.19 | 0.55 | -0.41 | 1.43 |
| | \mathcal{M}_4 | -19.97 | 12.46 | 10.12 | 15.70 |
| | \mathcal{M}_5 | 9.94 | 16.45 | 14.29 | -3.19 |
| | \mathcal{M}_6 | 19.99 | 6.21 | 3.71 | -14.25 |

To address the problem appearing in fit (II), we have enlarged in the total χ^2 the weight of the first wobbling band by a factor 10. This fitting strategy (III) can indeed improve the description of the first wobbling band as shown in Fig. 1. However, the wobbling energies of the second wobbling band are overestimated again in the low spin region.

In fitting strategy (IV), we take the full data collection as in fitting strategy (II), but keep fixed the LO parameters \mathcal{J}_k when performing the fit of \mathcal{M}_k at NLO. As can be seen, the description of the wobbling energies does not change much. However, as shown in Fig. 2, the agreement for the spin-rotational frequency relationships of the yrast band becomes a bit worse.

B. Wobbling bands in $^{161,165,167}\text{Lu}$

In Fig. 3, the wobbling energies as functions of spin I in $^{161,165,167}\text{Lu}$ as calculated at LO and NLO are shown in comparison with experimental data [23, 26, 27]. The results of

spin-rotational frequency relationships for their yrast and wobbling bands are displayed in Fig. 4. In the EFT calculations, the experimental data of the wobbling energies of the first wobbling band and the rotational frequencies of the yrast band are used to determine the parameters \mathcal{J}_k and \mathcal{M}_k . The obtained best-fit parameters for each Lu isotope are given in Table II.

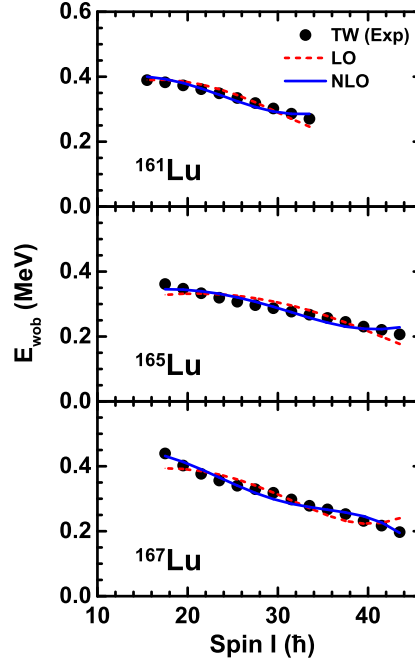


FIG. 3: (Color online) Wobbling energy as functions of spin in $^{161,165,167}\text{Lu}$ as calculated at LO and NLO in comparison with experimental data [23, 26, 27].

From Figs. 3 and 4, one can see that the EFT at LO and NLO can both reproduce this large amount of experimental data. In particular, the good agreement for the spin-rotational frequency relationships of the second wobbling band indicates that the EFT is quite efficient. The wobbling energies of these three nuclei decrease with spin I , thus exhibiting the feature of transverse wobbling. The descriptions at NLO are generally better than LO, which points to the relevance of the higher-order terms in the NLO Hamiltonian. In particular, the LO calculation shows an earlier termination of the transverse wobbling motion in ^{167}Lu . In addition, the LO calculation gives much smaller rotational frequencies at low spins, i.e., it overestimates the dynamical moment of inertia $dI/d\omega$.

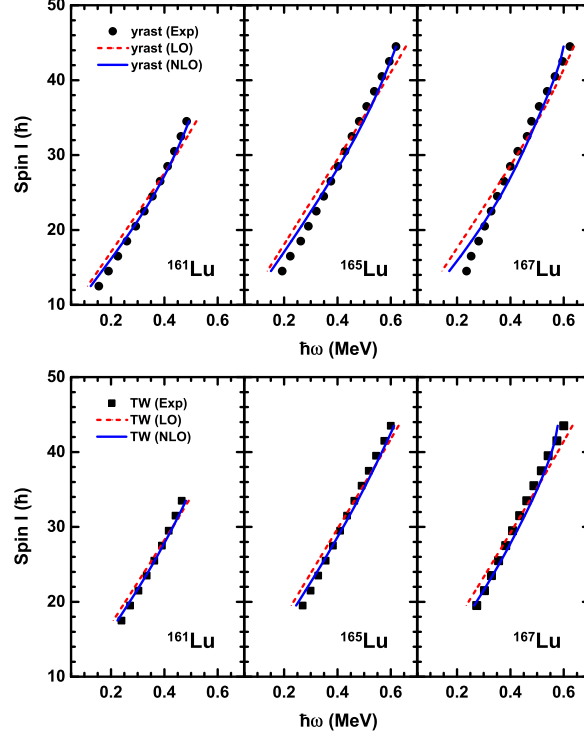


FIG. 4: (Color online) Spin-rotational frequency relationships for the yrast and wobbling bands in $^{161,165,167}\text{Lu}$ as calculated at LO and NLO in comparison with the experimental data [23, 26, 27].

C. Electromagnetic transitions

A hallmark of the wobbling mode on electromagnetic transition properties is the enhancement of the electric quadrupole component for $\Delta I = 1$ transitions between the neighboring wobbling bands. In Figs. 5 and 6, the $B(E2)_{\text{out}}/B(E2)_{\text{in}}$ and $B(M1)_{\text{out}}/B(E2)_{\text{in}}$ ratios for the transitions from the first wobbling band to the yrast band in $^{161,163,165,167}\text{Lu}$ as calculated at LO and NLO are shown in comparison with the available experimental data [24, 26, 27]. Here, “out” denotes the $\Delta I = 1$ inter-band transitions (wobbling \rightarrow yrast), and “in” refers to $\Delta I = 2$ intra-band transitions within the same wobbling band. Note that the results for ^{163}Lu have been obtained by fitting strategy (II), which gives the best agreement with the experimental wobbling energies and spin-rotational frequency relationships as shown in Figs. 1 and 2.

The large $B(E2)_{\text{out}}/B(E2)_{\text{in}}$ values and very small $B(M1)_{\text{out}}/B(E2)_{\text{in}}$ values support the occurrence of transverse wobbling motion in the Lu isotopes. Note that most of the

TABLE II: Parameters used in the LO and NLO calculations for $^{161,165,167}\text{Lu}$. The units of \mathcal{J}_k and \mathcal{M}_k are \hbar^2/MeV and \hbar^4/MeV^3 , respectively.

| | Nucleus | ^{161}Lu | ^{165}Lu | ^{167}Lu |
|-----|-----------------|-------------------|-------------------|-------------------|
| LO | \mathcal{J}_1 | 61.89 | 63.11 | 64.10 |
| | \mathcal{J}_2 | 49.53 | 55.52 | 52.10 |
| | \mathcal{J}_3 | 4.23 | 7.05 | 4.20 |
| NLO | \mathcal{J}_1 | 60.59 | 60.90 | 59.66 |
| | \mathcal{J}_2 | 44.61 | 50.04 | 43.17 |
| | \mathcal{J}_3 | 3.38 | 5.66 | 2.64 |
| | \mathcal{M}_1 | 9.99 | 9.96 | -10.00 |
| | \mathcal{M}_2 | 9.99 | 9.99 | 10.00 |
| | \mathcal{M}_3 | 0.05 | 0.14 | -0.38 |
| | \mathcal{M}_4 | -9.99 | -9.91 | -9.99 |
| | \mathcal{M}_5 | 3.03 | 0.92 | 8.92 |
| | \mathcal{M}_6 | 9.99 | 9.98 | 9.99 |

experimental $B(E2)_{\text{out}}/B(E2)_{\text{in}}$ values can be reproduced within error bars by the EFT both at LO and NLO.

In order to reproduce qualitatively the experimental values of $B(M1)_{\text{out}}/B(E2)_{\text{in}}$, we have quenched the relevant g -factor ($g_p - g_R$) in Eq. (38) by a factor 0.25. According to Ref. [43], such a quenching factor allows to take into account effects of the scissor mode, which mixes with the wobbling mode and could reduce the $B(M1)_{\text{out}}$ by a factor of 3-20.

IV. SUMMARY

The effective field theory for the collective motion of triaxially deformed nuclei has been generalized to odd-mass nuclei by including the angular momentum of the valence nucleon as an additional degree of freedom. The Hamiltonian has been constructed up to next-to-leading order, where it goes beyond the particle-rotor model by quartic terms. We have examined its applicability by calculating the wobbling bands in the lutetium isotopes $^{161,163,165,167}\text{Lu}$. It is found that by taking into account the NLO order corrections, the exper-

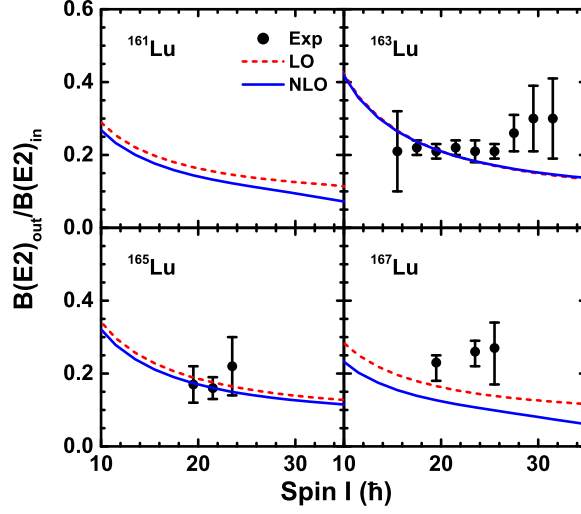


FIG. 5: (Color online) The $B(E2)_{\text{out}}/B(E2)_{\text{in}}$ ratio for the transitions from wobbling to yrast band in $^{161,163,165,167}\text{Lu}$ as calculated at LO and NLO in comparison with the available experimental data [24–27].

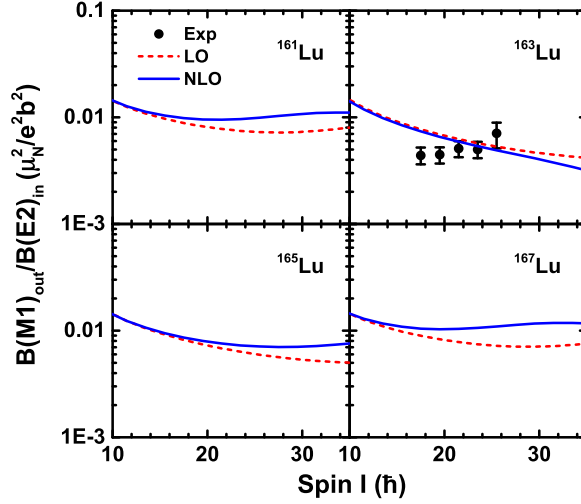


FIG. 6: (Color online) The $B(M1)_{\text{out}}/B(E2)_{\text{in}}$ ratio for the transitions from wobbling to yrast band in $^{161,163,165,167}\text{Lu}$ as calculated at LO and NLO in comparison with the available experimental data [24, 25].

imental wobbling energies and spin-rotational frequency relations are better described than at LO Hamiltonian, which points to the relevance of the higher-order terms in the NLO Hamiltonian. At the same time, the electromagnetic transition strengths for inter-band and

intra-band transitions are well described.

Next, we will further generalize the EFT by including the coupling of a proton and a neutron to the rotor and apply it to investigate chiral doublet bands [44].

Acknowledgements

This work has been supported in parts by Deutsche Forschungsgemeinschaft (DFG) and National Natural Science Foundation of China (NSFC) through funds provided by the Sino-German CRC 110 “Symmetries and the Emergence of Structure in QCD” (DFG Grant No. TRR110 and NSFC Grant No. 11621131001), the National Key R&D Program of China (Contract No. 2017YFE0116700 and No. 2018YFA0404400), and the NSFC under Grant No. 11935003. The work of U.-G.M. was also supported by the Chinese Academy of Sciences (CAS) through a President’s International Fellowship Initiative (PIFI) (Grant No. 2018DM0034) and by the VolkswagenStiftung (Grant No. 93562).

-
- [1] Q. B. Chen, N. Kaiser, U.-G. Meißner, and J. Meng, *Eur. Phys. J. A* **53**, 204 (2017).
 - [2] Q. B. Chen, N. Kaiser, U.-G. Meißner, and J. Meng, *Phys. Rev. C* **97**, 064320 (2018).
 - [3] U. van Kolck, *Phys. Rev. C* **49**, 2932 (1994).
 - [4] E. Epelbaum, H.-W. Hammer, and U.-G. Meißner, *Rev. Mod. Phys.* **81**, 1773 (2009).
 - [5] J. W. Holt, M. Kawaguchi, and N. Kaiser, *arXiv: nucl-th*, 1912.06055 (2019).
 - [6] C. Bertulani, H.-W. Hammer, and U. van Kolck, *Nucl. Phys. A* **712**, 37 (2002).
 - [7] H.-W. Hammer and D. Phillips, *Nucl. Phys. A* **865**, 17 (2011).
 - [8] E. Ryberg, C. Forssén, H.-W. Hammer, and L. Platter, *Phys. Rev. C* **89**, 014325 (2014).
 - [9] P. F. Bedaque and U. van Kolck, *Annu. Rev. Nucl. Part. Sci.* **52**, 339 (2002).
 - [10] H. Griebhammer, J. McGovern, D. Phillips, and G. Feldman, *Prog. Part. Nucl. Phys.* **67**, 841 (2012).
 - [11] H.-W. Hammer, A. Nogga, and A. Schwenk, *Rev. Mod. Phys.* **85**, 197 (2013).
 - [12] H. W. Hammer, S. König, and U. van Kolck, *arXiv: nucl-th*, 1906.12122 (2019).
 - [13] T. Papenbrock, *Nucl. Phys. A* **852**, 36 (2011).
 - [14] J. L. Zhang and T. Papenbrock, *Phys. Rev. C* **87**, 034323 (2013).

- [15] T. Papenbrock and H. A. Weidenmüller, Phys. Rev. C **89**, 014334 (2014).
- [16] T. Papenbrock and H. A. Weidenmüller, J. Phys. G: Nucl. Part. Phys. **42**, 105103 (2015).
- [17] T. Papenbrock and H. A. Weidenmüller, Phys. Scr. **91**, 053004 (2016).
- [18] E. A. Coello Pérez and T. Papenbrock, Phys. Rev. C **92**, 014323 (2015).
- [19] E. A. Coello Pérez and T. Papenbrock, Phys. Rev. C **92**, 064309 (2015).
- [20] E. A. Coello Pérez and T. Papenbrock, Phys. Rev. C **94**, 054316 (2016).
- [21] A. Bohr and B. R. Mottelson, *Nuclear structure*, vol. II (Benjamin, New York, 1975).
- [22] S. Frauendorf and F. Dönau, Phys. Rev. C **89**, 014322 (2014).
- [23] P. Bringel, G. B. Hagemann, H. Hübel, A. Al-khatib, P. Bednarczyk, A. Bürger, D. Curien, G. Gangopadhyay, B. Herskind, D. R. Jensen, et al., Eur. Phys. J. A **24**, 167 (2005).
- [24] S. W. Ødegård, G. B. Hagemann, D. R. Jensen, M. Bergström, B. Herskind, G. Sletten, S. Törmänen, J. N. Wilson, P. O. Tjøm, I. Hamamoto, et al., Phys. Rev. Lett. **86**, 5866 (2001).
- [25] D. R. Jensen, G. B. Hagemann, I. Hamamoto, S. W. Ødegård, B. Herskind, G. Sletten, J. N. Wilson, K. Spohr, H. Hübel, P. Bringel, et al., Phys. Rev. Lett. **89**, 142503 (2002).
- [26] G. Schönwaßer, H. Hübel, G. B. Hagemann, P. Bednarczyk, G. Benzoni, A. Bracco, P. Bringel, R. Chapman, D. Curien, J. Domscheit, et al., Phys. Lett. B **552**, 9 (2003).
- [27] H. Amro, W. C. Ma, G. B. Hagemann, R. M. Diamond, J. Domscheit, P. Fallon, A. Gorgen, B. Herskind, H. Hübel, D. R. Jensen, et al., Phys. Lett. B **553**, 197 (2003).
- [28] D. J. Hartley, R. V. F. Janssens, L. L. Riedinger, M. A. Riley, A. Aguilar, M. P. Carpenter, C. J. Chiara, P. Chowdhury, I. G. Darby, U. Garg, et al., Phys. Rev. C **80**, 041304(R) (2009).
- [29] J. T. Matta, U. Garg, W. Li, S. Frauendorf, A. D. Ayangeakaa, D. Patel, K. W. Schlax, R. Palit, S. Saha, J. Sethi, et al., Phys. Rev. Lett. **114**, 082501 (2015).
- [30] N. Sensharma, U. Garg, S. Zhu, A. D. Ayangeakaa, S. Frauendorf, W. Li, G. Bhat, J. A. Sheikh, M. P. Carpenter, Q. B. Chen, et al., Phys. Lett. B **792**, 170 (2019).
- [31] J. Timár, Q. B. Chen, B. Kruzsicz, D. Sohler, I. Kuti, S. Q. Zhang, J. Meng, P. Joshi, R. Wadsworth, K. Starosta, et al., Phys. Rev. Lett. **122**, 062501 (2019).
- [32] C. M. Petrache, P. M. Walker, S. Guo, Q. B. Chen, S. Frauendorf, Y. X. Liu, R. A. Wyss, D. Mengoni, Y. H. Qiang, A. Astier, et al., Phys. Lett. B **795**, 241 (2019).
- [33] Q. B. Chen, S. Frauendorf, and C. M. Petrache, Phys. Rev. C **100**, 061301(R) (2019).
- [34] S. Biswas, R. Palit, S. Frauendorf, U. Garg, W. Li, G. H. Bhat, J. A. Sheikh, J. Sethi, S. Saha,

- P. Singh, et al., Eur. Phys. J. A **55**, 159 (2019).
- [35] N. Sensharma, U. Garg, Q. B. Chen, S. Frauendorf, D. P. Burdette, J. L. Cozzi, K. B. Howard, S. Zhu, M. P. Carpenter, P. Copp, et al., Phys. Rev. Lett. **124**, 052501 (2020).
 - [36] S. Coleman, J. Wess, and B. Zumino, Phys. Rev. **177**, 2239 (1969).
 - [37] C. G. Callan, S. Coleman, J. Wess, and B. Zumino, Phys. Rev. **177**, 2247 (1969).
 - [38] L. D. Landau and E. M. Lifshitz, *Course of Theoretical Physics, Mechanics* (Pergamon Press, London, 1960).
 - [39] P. Ring and P. Schuck, *The nuclear many body problem* (Springer Verlag, Berlin, 1980).
 - [40] S. Y. Wang, B. Qi, and S. Q. Zhang, Chin. Phys. Lett. **26**, 052102 (2009).
 - [41] E. Streck, Q. B. Chen, N. Kaiser, and U.-G. Meißner, Phys. Rev. C **98**, 044314 (2018).
 - [42] Q. B. Chen, N. Kaiser, U.-G. Meißner, and J. Meng, Phys. Rev. C **99**, 064326 (2019).
 - [43] S. Frauendorf and F. Döna, Phys. Rev. C **92**, 064306 (2015).
 - [44] S. Frauendorf and J. Meng, Nucl. Phys. A **617**, 131 (1997).